

Divalent-dopant criterion for the suppression of Jahn-Teller distortion in Mn oxides: First-principles calculations and x-ray absorption spectroscopy measurements for Co in LiMnO₂

R. Prasad,¹ R. Benedek,² A. J. Kropf,² C. S. Johnson,² A. D. Robertson,³ P. G. Bruce,³ and M. M. Thackeray²

¹*Department of Physics, Indian Institute of Technology at Kanpur, Kanpur, 208016 India*

²*Chemical Technology Division, Argonne National Laboratory, Argonne, Illinois 60439, USA*

³*School of Chemistry, University of St. Andrews, St. Andrews, Fife, KY169ST United Kingdom*

(Received 2 April 2003; published 2 July 2003)

Co doping on the Mn sublattice of layered LiMnO₂ suppresses the Jahn-Teller-driven monoclinic distortion in favor of a layered rhombohedral structure. First-principles calculations (within the local-spin-density approximation–generalized-gradient approximation frame-work) using the VASP code, as well as x-ray absorption measurements, elucidate the effect of the Co doping on the atomic structure and the charge states of Mn and Co. The analogy between Li manganate and La manganite suggests that dopants of either system that are divalent in both the distorted antiferromagnetic phase and the symmetric ferromagnetic phase are most effective in suppressing the cooperative Jahn-Teller distortion.

DOI: 10.1103/PhysRevB.68.012101

PACS number(s): 61.66.Fn, 71.20.Nr

Li manganates are under intense scrutiny for their potential application as rechargeable lithium-battery-electrode materials.¹ The pronounced Jahn-Teller (JT) activity of Mn³⁺ ions, however, poses obstacles to the full exploitation of these promising materials. The Jahn-Teller activity is responsible for distortions of the MnO₆ octahedra in the orthorhombic² and (metastable) layered^{3,4} dioxides of composition LiMnO₂, as well as in the overlithiated spinel,⁵ Li₂Mn₂O₄. The magnitude of the cooperative Jahn-Teller distortion varies widely and discontinuously at structural phase transitions, during the redox cycles that accompany Li insertion/extraction. These variations often cause a breakup of the material, which is detrimental to the capacity and capacity retention of a battery. Efforts have therefore been made to suppress the cooperative Jahn-Teller distortion, e.g., by doping, with Co, Ni, or other elements. Doping LiMnO₂ with Co tends to form nonstoichiometric materials, with Li contents of 0.55–0.7, and stabilizes the rhombohedral ($R\bar{3}m$) symmetry,^{6–13} relative to the monoclinic structure, of LiMnO₂. Incidentally, theory predicts¹⁴ that Co doping also stabilizes the monoclinic structure relative to the orthorhombic structure, so that the stability order orthorhombic > monoclinic > rhombohedral is completely reversed upon Co doping.

In this paper, we investigate by first-principles computer simulation, and with x-ray absorption spectroscopy (XAS) measurements, the charge transfer between Mn and Co, which appears to play a critical role in the stabilization of the rhombohedral phase. A better understanding of the behavior of dopants such as Co and Ni in lithium manganates is expected to provide helpful guidance for future battery materials design. Ni doping of LiMnO₂, has also been found^{15–18} to stabilize the rhombohedral structure.

In addition to the dilution of Jahn-Teller-active Mn³⁺ ions by substitution of non-Mn atoms on the transition-metal sublattice, doping introduces atoms with different magnetic properties and oxidation states from those of the Mn host atoms. The significance of the dopant oxidation state and magnetic behavior was recently explored in the context of doped La manganites,¹⁹ which are analogous in some re-

spects to Li manganates, although the Mn-ion density is lower in the former, roughly proportional to the number of O atoms per formula unit.

Co and Ni impurities have been investigated in both lanthanum manganite and lithium manganate. To understand better their influence on the phase stabilities of the respective host materials, we explore the hypothesis that dopants in Mn³⁺ bearing oxides, with cooperative JT distortion, are most effective in promoting a high-symmetry crystal structure if they adopt a divalent state²⁰ in both the JT-distorted and the transformed structures. Previous analysis of dopant charge states has focused only on the transformed high-symmetry phase. The motivation for this criterion is that for each divalent dopant atom substitution, the resultant 4+ neighboring Mn ion is compatible (incompatible) with the undistorted (distorted) octahedral environment in the rhombohedral (monoclinic) structures of lithium manganate; a similar statement applies to the rhombohedral (orthorhombic) structures of lanthanum manganite. This is because Mn⁴⁺ stabilizes the (ferromagnetic) high-symmetry transformed phase by promoting double exchange²¹ or (ferromagnetic) superexchange,²² whereas Mn⁴⁺ destabilizes the (antiferromagnetic) low-symmetry untransformed phase with cooperative JT distortion, by interrupting the coupling along antiferromagnetic chains.

As divalent ions, Mg and Zn and possibly Co and Ni appear to be the most promising candidate dopants to stabilize the high-symmetry phases. Mg and Zn have been explored as dopants in LaMnO₃, and may merit consideration for LiMnO₂, however, transition metals may be even more favorable because of their compatibility with the ferromagnetism of the high-symmetry phase. Whether a given transition-metal dopant of LiMnO₂ (or LaMnO₃) adopts a divalent state, however, depends on a delicate balance between the ionization energy of Mn³⁺ and the energy gain by reduction of the dopant.²³ The local atomic environment plays a crucial role in determining this balance. First-principles local-density-functional theory enables predictions of both structural and electronic degrees of freedom, albeit with approximate treatment of electron exchange and correlation.

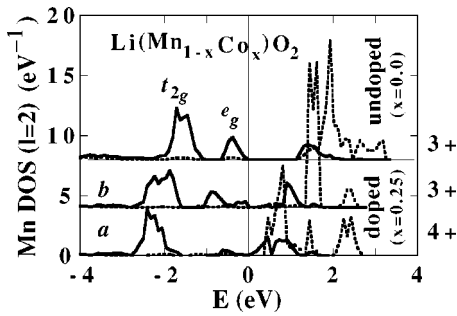


FIG. 1. Projected Mn-ion d -wave ($l=2$) density of electronic states in monoclinic $\text{LiMn}_{1-x}\text{Co}_x\text{O}_2$ for $x=0.0$ (top panel) and $x=0.25$ (bottom two panels). Calculations were performed with the VASP code. The full curve represents the majority-spin band and the dashed curve the minority-spin band. The zero on the abscissa corresponds to the Fermi energy. One of the three Mn atoms in the cell (labeled a) is oxidized to charge state $4+$, as indicated by the diminished weight of the e_g majority-spin band, while the Co atom is reduced to $2+$.

Calculations were performed with the VASP code,²⁴ based on the local-spin-density approximation–generalized-gradient approximation (LSDA-GGA), for $\text{LiMn}_{1-x}\text{M}_x\text{O}_2$, where $M=\text{Co}$ or Ni , at different dopant levels²⁵ x . The results indicate that, at small x , in either the monoclinic or the rhombohedral structures, Co is reduced and Mn is oxidized, relative to the average transition-metal charge state of $3+$. XAS measurements for nearly fully lithiated rhombohedral $\text{LiMn}_{1-x}\text{M}_x\text{O}_2$, with Co concentration $x=0.1$ are consistent with these predictions.

In the calculations described below, ferromagnetic and simple antiferromagnetic³¹ spin configurations were assumed. The invoked periodic-boundary conditions²⁴ imply ordering of Co on the transition-metal sublattice. We consider first the monoclinic structure, which can be synthesized by ion exchange.³⁴ The lower two panels in Fig. 1 show the d -wave-projected ($l=2$) spectra of electronic energies for Mn atoms in $\text{LiMn}_{0.75}\text{Co}_{0.25}\text{O}_2$, and, for comparison, the top panel shows the spectrum for Mn in LiMnO_2 . The unit cell contains 4 f.u. and four layers, with three Mn atoms and one Co atom in the transition-metal layer.³³ The (initial) antiferromagnetic configuration on the transition-metal sublattice was taken from Singh³¹ for the undoped system, in which up and down spins alternate along the atomic chains parallel to the monoclinic b axis. The converged self-consistent magnetic structures show a smaller (but nonzero) magnetic moment on Co than on Mn. The electronic energy spectra for the two symmetrically distinct types of Mn in the unit cell (we denote two of the Mn atoms as type a and one as type b) are shown in the bottom panels. The solid lines represent the majority carriers and the broken lines the minority carriers, and the zero on the abscissa is the Fermi energy. We note that the majority-spin spectra for Mn in the undoped system and for b -type Mn atoms in the doped system both have t_{2g} and e_g bands with similar weights. The a -type Mn atom, however, has a significantly attenuated e_g band. This behavior indicates charge transfer between the a -type Mn, which is oxidized to $4+$, and Co, which is reduced to $2+$, while the b -type Mn atoms remain in the $3+$ state. Other features of

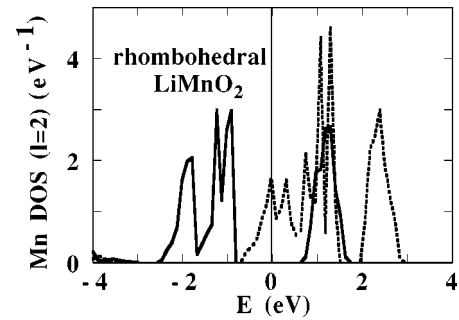


FIG. 2. Projected Mn-ion density of electronic states calculated for ferromagnetic LiMnO_2 in the rhombohedral structure. The full curve is the majority-spin band and the dashed curve is the minority-spin band. The zero on the abscissa corresponds to the Fermi energy.

the results are consistent with this interpretation. The octahedral stretching mode coordinate, Q_3 , of the oxygen octahedron, driven by the Jahn-Teller effect,³² is reduced to a value of 0.103 \AA for the a -type Mn, from a value $Q_3(0)=0.49 \text{ \AA}$ in the undoped system. The Q_3 values of the Co dopant and the b -type Mn are similar to $Q_3(0)$. Furthermore, the integrated d -electron count for Co atoms is about 0.5-electrons higher in the doped system than in rhombohedral LiCoO_2 . Calculations were also performed for monoclinic $\text{LiMn}_{1-x}\text{Co}_x\text{O}_2$ at $x=0.5$. In this case, no indication of charge transfer from Mn to Co is observed. Therefore, for the (hypothetical) monoclinic $\text{LiMn}_{1-x}\text{Co}_x\text{O}_2$, charge transfer is predicted to occur only over a certain range of doping.

The rhombohedral phase was assumed to be ferromagnetic, which has been observed experimentally for Ni-doped systems at low temperatures.³⁴ We note also that Co doping of the perovskite LaMnO_3 transforms the antiferromagnetism of the host to a ferromagnetic structure.¹⁹ In the LSDA-GGA calculations for the ferromagnetic (unlike the antiferromagnetic) case, the rhombohedral structure is stable, however, surprisingly, the Mn ions adopt a low-spin configuration, as illustrated in Fig. 2. It is seen in this figure that, instead of a filled lower level of a split majority e_g band, which occurs in the high-spin Mn^{3+} state, the minority t_{2g} band is partially filled. In calculations for the rhombohedral structure at $x=0.25$, the results suggest charge transfer from Mn to Co. The bottom panel of Fig. 3, similar to results in Fig. 2, shows the Mn minority band straddling the Fermi energy. The Co dopant (cf. middle panel of Fig. 3) shows a large spin splitting, in sharp contrast to the spectra for Co in rhombohedral LiCoO_2 . As a result of this spin splitting, the dopant majority band, as well as most of the minority t_{2g} band, are occupied, which indicates at least partial transfer of charge from Mn to Co. Another indication of charge transfer is the lengthened Co-O bond lengths of 2.05 \AA in LiMnO_2 , compared to values of 1.93 \AA in LiCoO_2 , which imply Co-ion reduction. Note that the calculations predict a high-spin configuration for Co, in contrast to its behavior in LiCoO_2 .

The electronic spectra of rhombohedral LiMnO_2 (Fig. 2) exhibits half-metallic behavior, with a large density of electronic states at the Fermi level in the minority band and a gap in the majority band. The calculations also predict metallic

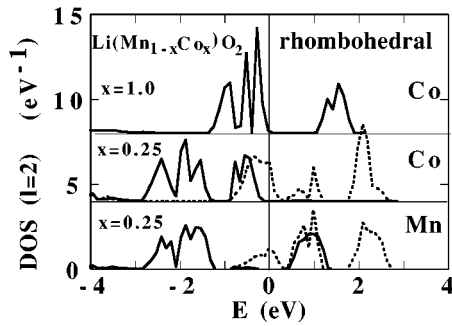


FIG. 3. Projected ($l=2$) Mn-ion (bottom panel) and Co-ion (middle panel) density of electronic states calculated for the ferromagnetic state of rhombohedral $\text{LiMn}_{0.75}\text{Co}_{0.25}\text{O}_2$. The full curves are the majority-spin bands and the dashed curves the minority-spin bands. The zero on the abscissa corresponds to the Fermi energy. For comparison, the top panel shows the density of states for paramagnetic rhombohedral LiCoO_2 .

behavior for the cobalt-doped system with $x=0.25$. If Co-doped rhombohedral LiMnO_2 were indeed metallic, the metallic screening would likely attenuate the charge transfer between Mn and Co. Since the LSDA-GGA calculations predict metallic behavior for the rhombohedral structure, we would not expect the charge transfer to be as robust as in the monoclinic structure (Fig. 1), for which the predicted energy spectra appear only to be semimetallic. Co doping of LaMnO_3 , incidentally, increases polaronic conductivity but does not result in metallic behavior.¹⁹ No electronic transport measurements on $\text{LiMn}_{1-x}\text{Co}_x\text{O}_2$ appear to have been done, but it seems likely that the material is insulating.

We have seen that LSDA-GGA calculations, based on assumed magnetic configurations, predict charge transfer from Mn to Co in both the monoclinic and rhombohedral phases of $\text{LiMn}_{1-x}\text{Co}_x\text{O}_2$. The approximations employed in the calculations, however, make experimental tests highly desirable. X-ray and photoemission spectroscopies on doped LaMnO_3 demonstrate charge transfer from Mn to Co.^{23,35-37}

In Fig. 4 are presented K -edge XAS spectra, measured at the Argonne National Laboratory Advanced Photon Source³⁸ (APS) for Co in $\text{Li}_{1-y}\text{Mn}_{0.9}\text{Co}_{0.1}\text{O}_2$, where $y=0.17$ as well as for trivalent Co in LiCoO_2 and divalent Co in CoO . The specimens, with structural symmetry $R\bar{3}m$, were synthesized by an ion-exchange procedure, which yielded a lithium-deficient system; this was followed by electrochemical lithiation to achieve nearly full occupancy on the Li sublattice.^{12,39} An interpretation of the near-edge structural features for Co absorption in LiCoO_2 has been presented previously.⁴⁰ Significant for the oxidation state assignment is the dipole-allowed onset edge in the region 7.715–7.718 keV. The spectrum for $\text{LiMn}_{0.9}\text{Co}_{0.1}\text{O}_2$ lies close to that for the divalent standard, CoO , and well below the trivalent standard, LiCoO_2 which is shifted to higher energy by about 2 eV. Spectra for the Mn K -edge (not shown) of $\text{LiMn}_{0.9}\text{Co}_{0.1}\text{O}_2$ are proximal to those for a trivalent Mn_2O_3 standard; at the low dopant concentration employed, the

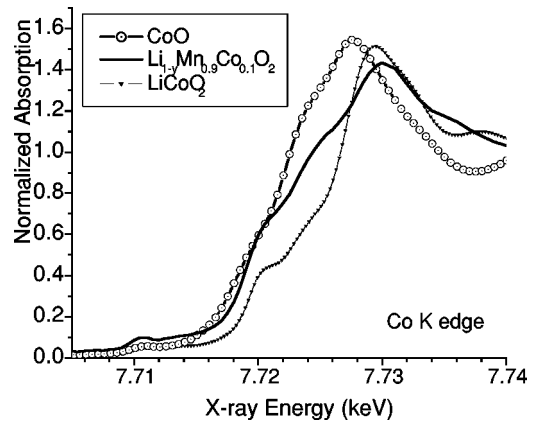


FIG. 4. XAS K -edge spectra for Co in $\text{Na}_{0.012}\text{Li}_{1-y}\text{Mn}_{0.901}\text{Co}_{0.094}\text{O}_2$, with $y=0.17$ and in reference divalent (CoO) and trivalent (LiCoO_2) oxide systems. The Co-doped specimen was obtained by discharging in an electrochemical cell a specimen with composition $\text{Na}_{0.012}\text{Li}_{0.642}\text{Mn}_{0.901}\text{Co}_{0.094}\text{O}_2$, obtained by ion exchange (Ref. 12). Spectra for the Co-doped system are close to those of the divalent CoO , and shifted to lower energy relative to undoped LiCoO_2 , in the region near the edge onset at about 7.715 keV.

slight shift anticipated for the Mn K -edge towards that of a quadrivalent standard (Li_2MnO_3) is difficult to detect. Nevertheless, the presence of Co^{2+} clearly implies an equal concentration of Mn^{4+} .

We have asserted that dopants that are divalent in *both* a JT-distorted antiferromagnetic phase and in a ferromagnetic phase of higher symmetry are effective in stabilizing the latter. This is because the resultant Mn^{4+} ions act to destabilize one and stabilize the other. In this work, first-principles calculations with the VASP code predict that Co dopants are divalent in both the monoclinic and the rhombohedral phases of $\text{LiMn}_{1-x}\text{Co}_x\text{O}_2$ at $x=0.25$. Co K -edge XAS measurements for a specimen with $x=0.1$ exhibit a divalent state, or one considerably reduced relative to a trivalent state. We believe that the divalent-dopant criterion for the suppression of the JT distortion in Mn-oxides, although not subject to rigorous proof, is at least a useful working hypothesis to guide the search for suitable dopants, and first-principles calculations provide a convenient tool for screening candidate dopants.

This work was supported at Argonne National Laboratory by the chemical sciences division of the Office of Basic Energy Sciences of the U.S. Department of Energy, under Contract No. W31-109-Eng-38, and at the Indian Institute of Technology, Kanpur, by the department of science and technology, New Delhi, under Project No. SP/S2/M-51/96. Most of the computational work was performed at the National Energy Research Supercomputer Center. The work performed at the MRCAT of the Advanced Photon Source is supported in part by funding from the Department of Energy under Grant No. DEFG0200ER45811, and by the U.S. Department of Energy, Office of Science, Office of Basic Energy Sciences, under Contract No. W-31-109-Eng-38.

- ¹J.-M. Tarascon and M. Armand, *Nature (London)* **414**, 359 (2001).
- ²J. E. Greedan, N. P. Raju, and I. J. Davidson, *J. Solid State Chem.* **128**, 209 (1997).
- ³A. R. Armstrong and P. G. Bruce, *Nature (London)* **381**, 499 (1996).
- ⁴E. Capitaine, P. Gravereau, and C. Delmas, *Solid State Ionics* **89**, 197 (1996).
- ⁵W. I. F. David, J. B. Goodenough, M. M. Thackeray, and M. G. S. R. Thomas, *Rev. Chim. Miner.* **20**, 636 (1983).
- ⁶A. R. Armstrong, R. Gitzendanner, A. D. Robertson, and P. G. Bruce, *Chem. Commun. (Cambridge)* **17**, 1833 (1998).
- ⁷A. R. Armstrong, A. D. Robertson, R. Gitzendanner, and P. G. Bruce, *J. Solid State Chem.* **145**, 549 (1999).
- ⁸A. R. Armstrong, A. D. Robertson, and P. G. Bruce, *Electrochim. Acta* **45**, 285 (1999).
- ⁹P. G. Bruce, A. R. Armstrong, and R. L. Gitzendanner, *J. Mater. Chem.* **9**, 193 (1999).
- ¹⁰A. D. Robertson, A. R. Armstrong, and P. G. Bruce, *Chem. Commun. (Cambridge)* **20**, 1997 (2000).
- ¹¹A. D. Robertson, A. R. Armstrong, A. J. Fowkes, and P. G. Bruce, *J. Mater. Chem.* **11**, 113 (2001).
- ¹²A. D. Robertson, A. R. Armstrong, and P. G. Bruce, *Chem. Mater.* **13**, 2380 (2001).
- ¹³A. R. Armstrong, A. J. Paterson, A. D. Robertson, and P. G. Bruce, *Chem. Mater.* **14**, 710 (2002).
- ¹⁴G. Ceder and S. K. Mishra, *Electrochem. Solid-State Lett.* **2**, 550 (1999). The influence of various dopants on the relative stability of the orthorhombic and monoclinic forms of LiMnO_2 is discussed in this paper.
- ¹⁵T. E. Quine, M. J. Duncan, A. R. Armstrong, A. D. Robertson, and P. G. Bruce, *J. Mater. Chem.* **10**, 2838 (2000).
- ¹⁶J. Reed and G. Ceder, *Electrochem. Solid-State Lett.* **5**, A145 (2002).
- ¹⁷T. Ohzuku and Y. Makimura, *Chem. Lett.* **8**, 744 (2001).
- ¹⁸Z. Lu, D. D. McNeil, and J. R. Dahn, *Electrochem. Solid-State Lett.* **4**, A191 (2001). This paper discusses the stabilizing properties of Ni^{2+} in a slightly different context from the present work.
- ¹⁹S. Hebert, C. Martin, A. Maignan, R. Retoux, M. Hervieu, N. Nguyen, and B. Raveau, *Phys. Rev. B* **65**, 104420 (2002).
- ²⁰To simplify the discussion, only the oxidation states of the transition metals are considered here, although oxygen also participates in the charge transfer when vacancies or impurities are introduced. G. Ceder, M. K. Aydinol, and A. F. Kohan, *Comput. Mater. Sci.* **8**, 161 (1997).
- ²¹P. G. de Gennes, *Phys. Rev.* **118**, 141 (1960).
- ²²I. O. Troyanchuk, L. S. Lobanovsky, D. D. Khalyavin, S. N. Pastushonok, and H. Szymczak, *J. Magn. Magn. Mater.* **210**, 63 (2000).
- ²³J. H. Park, S. W. Cheong, and C. T. Chen, *Phys. Rev. B* **55**, 11 072 (1997).
- ²⁴G. Kresse and J. Furthmüller, *Comput. Mater. Sci.* **6**, 15 (1996); *Phys. Rev. B* **54**, 11 169 (1996).
- ²⁵For computational convenience, most of calculations were performed at a dopant concentration $x=0.25$. The critical concentration $x_{cr}(T)$, above which the rhombohedral structure is stabilized at temperature T , is difficult to measure precisely, or predict theoretically. The employed synthesis route (Refs. 6–13), which involves ion exchange, typically yields specimens with a lithium deficiency, a small amount of residual Na, and associated transition-metal vacancies. Obstacles to accurate theoretical prediction of $x_{cr}(T)$ include (i) uncertainty in the magnetic structures (Ref. 26), even for the undoped system; (ii) uncertainty in the Co-dopant distribution; and (iii) difficulty in correcting first-principles calculations for nonzero temperature. Although the treatment of electron correlation in transition-metal oxides within the LSDA-GGA has well-known shortcomings (Ref. 27), this framework does yield realistic atomic structures and correct relative stabilities of the undoped lithium manganese oxides (Ref. 28). Calculations related to $x_{cr}(0)$ are presented elsewhere (Refs. 29 and 30).
- ²⁶Y. I. Jang, F. C. Chou, and Y. M. Chiang, *J. Phys. Chem. Solids* **60**, 1763 (1999).
- ²⁷O. Bengone, M. Alouani, P. Blöchl, and J. Hugel, *Phys. Rev. B* **62**, 16 392 (2000).
- ²⁸S. K. Mishra and G. Ceder, *Phys. Rev. B* **59**, 6120 (1999).
- ²⁹A. I. Landa, C. C. Chang, P. N. Kumta, L. Vitos, and I. A. Abrikosov, *Solid State Ionics* **149**, 209 (2002).
- ³⁰R. Prasad and R. Benedek (unpublished).
- ³¹D. J. Singh, *Phys. Rev. B* **55**, 309 (1997).
- ³²C. A. Marianetti, D. Morgan, and G. Ceder, *Phys. Rev. B* **63**, 224304 (2001).
- ³³The 16-atom-cell calculations utilized a set of 36 special k points generated with Monkhorst-Pack indices (4,4,4). For each structure (monoclinic or rhombohedral) and magnetic configuration (ferromagnetic or antiferromagnetic), the internal coordinates were relaxed to minimize the Hellmann-Feynman forces, and the cell coordinates were relaxed to minimize the pressure and the stress tensor.
- ³⁴M. E. Spahr, P. Novak, Bernhard Schnyder, O. Haas, and R. Nesper, *J. Electrochem. Soc.* **145**, 1113 (1998).
- ³⁵J. van Elp, *Phys. Rev. B* **60**, 7649 (1999).
- ³⁶J. H. Park, *Phys. Rev. B* **60**, 7651 (1999).
- ³⁷LSDA calculations for Co-doped LaMnO_3 are also suggestive of charge transfer. Z. Yang, L. Ye, and X. Xie, *Phys. Rev. B* **59**, 7051 (1999).
- ³⁸The spectra were taken at the MRCAT insertion device beamline at the Argonne National Laboratory APS. See C. U. Segre, N. E. Leyarowska, W. M. Lavender, P. W. Plag, A. S. King, A. J. Kropf, B. A. Bunker, K. M. Kemner, P. Dutta, R. S. Duran, and J. Kaduk, in *Synchrotron Radiation Instrumentation*, edited by P. Pianetta, J. Arthur, and S. Brennan (American Institute of Physics, New York, 2000), p. 419.
- ³⁹A. Robertson and P. G. Bruce (unpublished).
- ⁴⁰W. S. Yoon, K. K. Lee, and K. B. Kim, *J. Electrochem. Soc.* **147**, 2023 (2000).